

Electrification of wind-blown sand: Recent advances and key issues

Xiao-Jing Zheng^{1,2,a}

¹ Key Laboratory of Mechanics on Western Disaster and Environment, Lanzhou University, Lanzhou, 730000, China

² College of Civil Engineering and Mechanics, Lanzhou University, Lanzhou, 730000, China

Received 31 January 2013 and Received in final form 16 June 2013

Published online: 11 December 2013 – © EDP Sciences / Società Italiana di Fisica / Springer-Verlag 2013

Abstract. In this paper, we summarize the recent advances on the electrification of wind-blown sand. Some of the outstanding questions, such as the interpretation of the electrification of wind-blown sand, measurements on and models of the features of the wind-blown sand E -fields, as well as their effect on the wind-blown sand flux and electromagnetic wave propagation, are reviewed. We end by highlighting the challenges that remain.

1 Introduction

In natural granular flows, such as wind-blown sand flows [1,4,5], snowstorms [2,6], volcanic plumes [3,7] etc., the existence of electrostatic charges has been widely acknowledged and has become an increasingly active area of research in recent years. Electric fields in wind-blown sand flows, dust storms and dust evils could be as strong as several kilovolts per metre which may introduce flashover and breakdown of transmission lines [8], attenuation (or even interruption) of electromagnetic wave propagation [9], etc. The electrification of wind-blown sands and dusts brought the “corona effect” to military helicopters operating in desert conditions, generating distinctive glowing rings along the metal rotor blades (fig. 1a) and thus making the aircraft more visible to the enemy [10]. On other planets, such as Mars, electric dust devils could make the particles on the surface saltate or leave the surface with little force in the wind, and also significantly affect the work of the Mars Exploration Rover [11,12]. Similarly, electric ash plumes over erupting volcanoes (figs. 1b and c) have been known to generate lightning flashes which could pose a risk to air traffic [13,14]. Due to the wide range of spatial scales, the complex surface conditions, the diversity of particle sizes and the geometric shapes involved in these phenomena, the electrification of sand particles, combined with wind-blown sand flows, is still poorly understood. Therefore, it is important to make in-depth investigations into the mechanism and influence of the electrification of wind-blown sand, so as to effectively prevent resultant damage.

Since the beginning of the last century, numerous scholars have attempted to understand the mystery of

the electrification of wind-blown sand utilizing a variety of methods and aspects, including field and wind-tunnel measurements, theoretical analysis on the particle-charging mechanism, and quantitative predictions derived from theoretical models. A general consensus has been reached that the E -field of wind-blown sand is produced by moving sand particles with opposite electric polarity, where the polarity is somehow related to the size of the sand particles [4,15–17]. However, owing to the complex mechanism and the influence of the electrification of wind-blown sand [18], a number of issues remain poorly understood. These include: 1) why sand particles get charged during wind-blown sand movements; 2) how many electric charges a sand particle acquires; 3) why the electric polarity of sand particles is related to the particles' size; 4) what the change law of wind-blown sand E -fields is, and 5) how to predict the intensity and influence of wind-blown sand E -fields. The difficulties in understanding may arise on the one hand from unclear recognition of the features of the turbulent flows in the atmospheric boundary layer (which has a high Reynolds number up to 10^6), and on another hand from the complexity generated by various modes of sand particle motions with diverse particle sizes on/above different surface conditions, such as collision, splash, creep, saltation and suspension, etc. More importantly, all of these motions are directly related to wind field, atmospheric conditions, geographical environment, biological vegetation, physical-chemical factors, etc. Therefore, the electrification of wind-blown sand is a typical complex system characterised by nonlinearity, randomness, multi-field coupling between thermal diffusion, E -fields and sand movements, as well as trans-scale processes with multi-phase media.

This paper attempts to introduce and review the fundamental laws of the electrification of wind-blown sand

^a e-mail: xjzheng@lzu.edu.cn

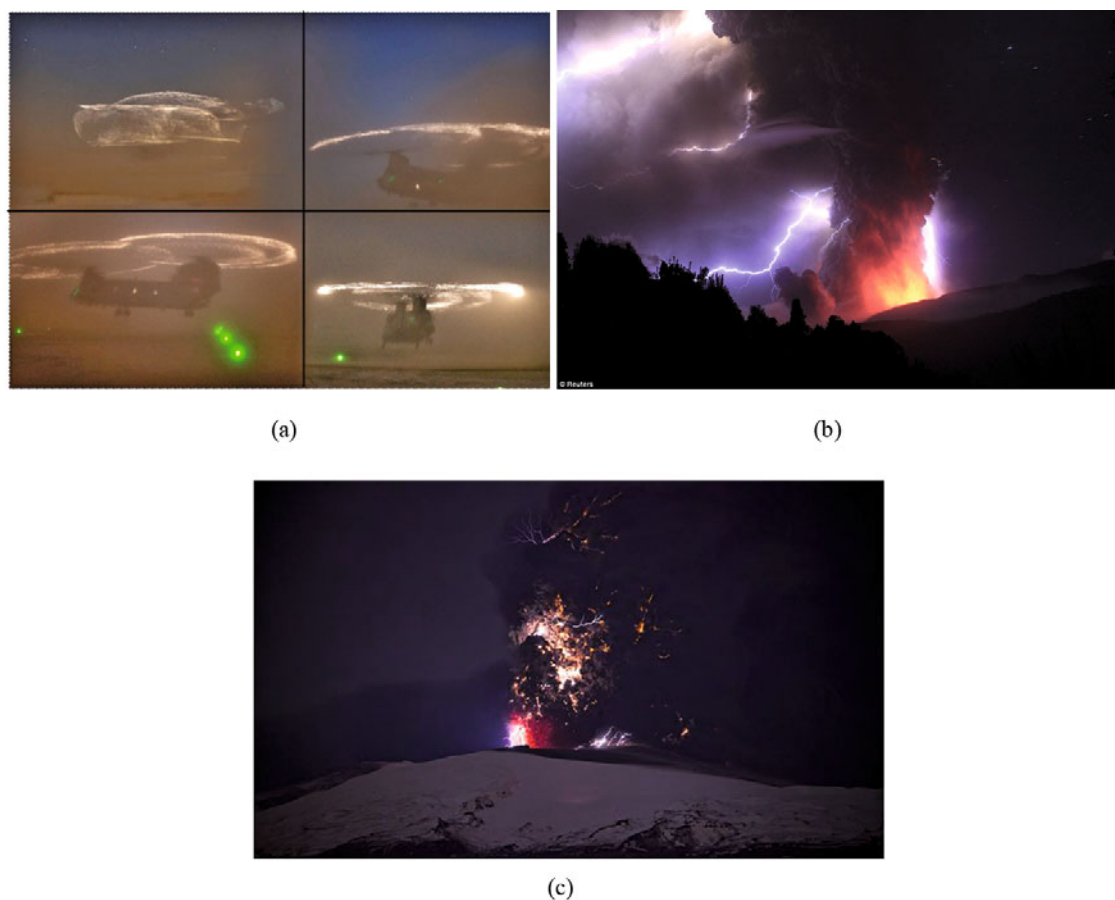


Fig. 1. Electric phenomena associated with dusty environments: (a) the “corona effect” along metal rotor blades of military helicopters when landing/slowing down near to the ground in deserts, the numerous small sparks can be explained by grains of sand striking a normally operating rotor blade (photos by Michael Yon) [10]; (b) and (c): lightning flashes generated by an electric ash plume over erupting volcanoes in Puyehue-Cordon Caulle, Chile and Reykjavik, Iceland, respectively [13,14]. Figures reprinted from Michael Yon, © Reuters, and Oli Haukur Myrdal, with kind permission.

and their influence, with later discussion directed to the challenges remaining in this field. It will begin with a brief review of existing experimental measurements and the contact charging mechanism of sand particles in sect. 2; sect. 3 summarises experimental and theoretical studies on the E -fields generated by wind-blown sand movements; sect. 4 describes the influence of the E -fields produced by charged sands, with particular emphasis on the influence of wind-blown sand flux and the propagation of electromagnetic waves; and finally, sect. 5 attempts to delineate the prospects for future progress and some challenging issues that remain poorly understood.

2 Experimental measurements and contact charging mechanism of sand particles

2.1 Experimental measurements

C.E.S. Phillips is perhaps the first scholar who conducted experimental studies on the contact charging of sand particles. His experiments found that when sand particles

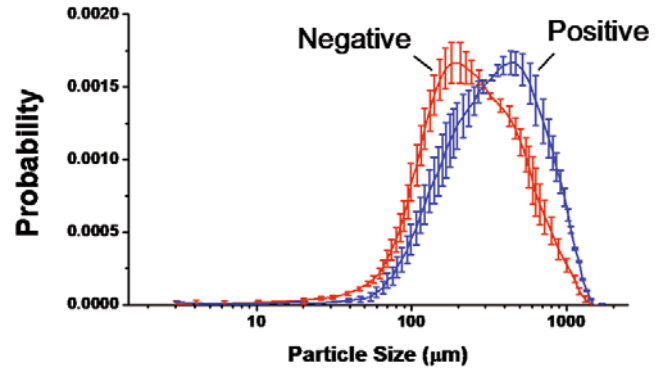
sampled from the Sahara Desert slid down an inclined tin-plane, sand-plane and wood-plane respectively, they became negatively charged while the inclined planes all exhibited a net positive charge [19]. Later on, W.A.D. Rudge found that larger sand particles were positively charged and smaller particles were negatively charged when the sand particles were sputtered with an air jet [20]. Other scientists verified this result [4,16,21,22]. It is interesting that in snowstorms, larger snow particles are also found to be positively charged and smaller ones negatively charged [2,23]. Similarly, when water drops collide with an ice surface, the splashed water droplets acquire negative charges while the ice surface becomes positively charged [24]. It should be noted that the conclusion concerning the charge polarity is based on statistical analysis and that the charge-to-mass ratio used to characterise the charges of the sand particles is the average charge per unit mass. Generally, the charge-to-mass ratio can be obtained by measuring the total charges and mass during a certain period of time. Sand particles are collected using a Faraday cage (cup) or similar equipment, then the total charge and mass of the collected particles can be measured using

Table 1. Experimental results of charge-to-mass ratios in wind-blown sand flux.

| Reference | Charge-to-mass ratio ($\mu\text{C kg}^{-1}$) | Diameter (μm) | Wind velocity (height) (m s^{-1}) |
|--|---|-------------------------------|---|
| Schmidt <i>et al.</i> [5] (Field) | 66 | 250 | 7 (1.5m) |
| Zheng <i>et al.</i> [15] (Wind-tunnel) | $-124 \div 0.95$ | $0 \div 1000$ | $7 \div 20$ (0.45m) |
| Qu <i>et al.</i> [29] (Wind-tunnel) | $-304 \div 158$ | $80 \div 315$ | $8 \div 22$ (0.3m) |
| Zhang <i>et al.</i> [31] (Wind-tunnel) | $-24.3 \div 65.8$ | $100 \div 600$ | $8 \div 22$ (0.3m) |
| Fuerstenau and Wilson [25] (Field) | $-3.5 \times 10^7 \div 3.8 \times 10^7$ | $0.4 \div 50$ | – |

an electrometer and a balance, respectively [5, 16, 25, 26]. Table 1 lists recent experimental results of charge-to-mass ratios which vary over a wide range. In addition, it also implies that particle size and wind velocity have a strong influence on the charge-to-mass ratio. In general, smaller particles exhibit larger charge-to-mass ratios, ranging up to $10^7 \mu\text{C kg}^{-1}$ for particles of $0.4 \div 50 \mu\text{m}$ [25]. This is because small particles have small mass while the charges are equal during charge transfer between large and small particles in wind-blown sand flows. Moreover, it has been reported that the charge-to-mass ratio increases with wind-velocity at the same height, but decreases with height at the same velocity [15]. This observation could be explained by the decrease of the average grain size and concentration with height at the same velocity, and their increase with wind velocity at the same height. Certainly, this discussion is based on the assumption that when large and small particles contact and separate, the generated charges are the same in magnitude but opposite in polarity [4, 15, 17, 18, 27]. Furthermore, wind-tunnel data show that near the surface, the charge-to-mass ratio is positive when the wind velocity is anywhere up to 20 m s^{-1} [15], which agrees with field experiments [5]. This may be due to the increase of the percentage of large particles lifted into the saltation layer due to the increase of wind velocity. The changing laws of the charge-to-mass ratio with wind velocity and height are not only suitable for a “uniform” sand bed (the size distribution is very narrow), but also for a “mixed” sand bed (the size distribution is relatively wide). However, the measured charge-to-mass ratio of a “mixed” sand bed is much bigger than that of a “uniform” sand bed [15]. This might be caused by charge segregation depending on the relative size difference between particles [28].

Another unanswered question is whether there exists a critical particle size for sand particles’ charge polarity. NASA scientists gave a critical diameter of $60 \mu\text{m}$ derived from wind-tunnel experiments [21]. Zheng *et al.* [15] reported quite a different result about the sign of electric charges based on experiments in a field environmental wind-tunnel with a “uniform” sand bed sampled from a sand dune at the southeastern edge of the Tengger Desert, viz. negative charge is gained when the diameter is smaller than $250 \mu\text{m}$ and positive charge is gained if the diameter is larger than $500 \mu\text{m}$. Therefore it would appear that there exists a critical range rather than a particular value of particle size for the charge polarity, in statistical sense. Recently, Forward *et al.* [22] provided experimental evidence for Zheng *et al.*’s conclusion that i) the size of neg-

**Fig. 2.** Particle size distribution of negatively charged (red) and positively charged (blue) particles (edited from Forward *et al.* [22]).

atively charged (red) and positively charged (blue) particles follows a single-peak distribution and ii) the size of negatively charged particles tends to be smaller than the positively charged particles (as shown in fig. 2). Of course, the critical particle size for the charge polarity of sand particles is related to the incoming wind velocity, height from sand surface and particle size, as well as the size distribution of the sample particles.

Difference may also arise from the measuring method, since in traditional experiments a Faraday cup is used as a sand tray to collect positive and negative charged sand particles together, which might underestimate the charges for a long-time run due to the charge neutralisation within the Faraday cup. As an improvement, the author’s group designed a real-time measurement system including a Faraday cup to receive sand particles, an electrometer to record real-time electric charges and a barrel to measure the weight. Such an instrument offers a promising means of more accurate measurement of the real-time charge-to-mass ratio in field observations and wind-tunnel experiments. Figure 3 shows the real-time results of charge-to-mass ratios measured at 5 cm above the ground in field observations, which are higher than the wind-tunnel data [15].

Even so, the problem of charge neutralisation still exists. Due to the resolution of instruments and the difficulty of capturing an undisturbed single sand particle, most of existing studies on the electric charge and polarity of sand particles in wind-blown sand flux are based on some sort of inference together with a few experimental results of

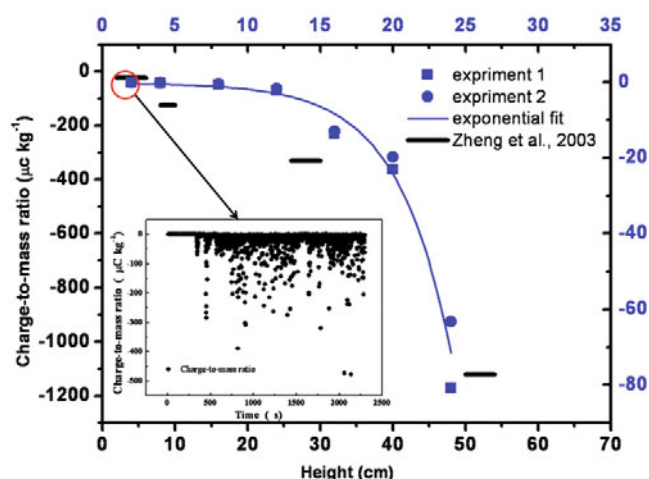


Fig. 3. A comparison between field observational and wind-tunnel data [15]. Insert image demonstrates the average charge-to-mass ratio evolving with time.

the electricity and polarity of sand grains after a single collision. For example, based on the theoretical analysis of the attenuation of electromagnetic wave propagation in dust storms, Zhou *et al.* [30] inferred that the suspending sand particles have negative charges which are partially distributed on the sand surface. However, charge transfer after a single collision has a distinct character from that observed in wind-blown sand flux. Therefore, more convincing experimental evidence relating to the charges and polarity of a single particle moving in a wind-blown sand flux, as well as accurate measurement methods and apparatus, are needed to fully resolve this issue.

2.2 Contact charging mechanism

In addressing the question of why the charge polarity is related to the particle's size, Latham [23] and Henry [32] gave an asymmetric collision explanation, that is, the difference of the contact area during a collision between a small and a large particle results in a temperature-gradient between the small particle and the larger one, which impels charge transfer between them. Some scholars suggested that the transfer ion species might be H^+ and OH^- provided by the "water bridge" (as shown in fig. 4), and humidity and atmospheric pressure could affect the electric charge on the insulating surface [33–35]. The temperature-gradient theory can also be applied to explain the electrification of snow particles whose electric charges also depend on particle size [2,27]. However, as a theoretical interpretation of particle-size-dependent bipolar charging, the temperature-gradient theory has not been verified by experiments due to the difficulty of measuring the instantaneous temperature difference between the contact particles. Moreover, it remains to be verified whether the instantaneous temperature difference is enough to impel the ion transfer between sand particles.

Because of the difficulty of directly and precisely measuring the electrification of sand particles, the contact

charging mechanism still remains at the speculations and hypothesis stage, which can be generally divided into 7 classes (as listed in table 2) [36]. They include: 1) cleavage/fractoelectrification; 2) bombardment charging (photons, charging particles); 3) pyroelectric charging; 4) piezoelectric and electret effect charging; 5) polarization by Earth's atmospheric electric field; 6) triboelectric charging and 7) contact electrification.

Conjectures 1)-5) are plausible, but they may play a non-definitive role in sand particles' charging. Firstly, in conjecture 1), cleavage of sand particles requires large impact energy to break a sand particle, which cannot be provided during the sand bed collisions process in wind-blown sand flux. Secondly, sand particles may be charged due to solar wind bombardment or photoelectron ejection from a sunlit surface [37,38], but speculation 2) cannot explain why larger sand particles acquire positive charges and smaller ones acquire negative charges. Thirdly, for speculations 3) and 4), the temperature gradient caused by heating can lead to the Thomson effect, however this is a second-order effect that can be negligible [39]. Meanwhile, Peterson [40] pointed out that the piezo-electric contribution to the charging of a sand particle is less than 20 percent of its total charges, therefore the piezo-electric effect is not an important factor; For speculation 5), the electric charges polarised by Earth's atmospheric electric field could be very tiny since the fair weather electric field is only 120 V m^{-1} , and this effect could therefore also be negligible. Therefore, the most likely mechanisms are conjectures 6) and 7), *i.e.*, tribo-electrification and contact electrification. It should be noted that friction and collision are two different types of contact types between sand particles' surfaces [8]. For friction, the frictional distance affects the electric charges more than the friction velocity [41,42]. Lowell and Rose-Innes [43] pointed out that rubbing is not necessary, and mere contact is sufficient to cause the transfer of considerable charge. Therefore, speculations 6) and 7) together are thought to be the contact electrification mechanism of sand particles' charging, and have attracted increasing interests from researchers in the field [17,18,44–48].

For the contact electrification mechanism, there are two kinds of contact charging models that explain the electrification of sand particles, *i.e.*, the asymmetric contact charging model and the contact potential difference model. The former has been established based on work function theory [15,17,49], for instance, Kok and Renno [16] proposed an effective contact potential difference between pairs of similar composition but different sizes, and explained why larger particles are charged positively and smaller particles are charged negatively. The latter is based on the high-energy trapped charged species theory [41], with the assumption that there are two surface states in the insulator surfaces, *i.e.* high-energy and low-energy states. As illustrated in fig. 5, when two particles come into contact with each other, charged species may be trapped in the high-energy states on one surface and relaxed to low-energy states on the other surface, and after the species relax to their low-energy states they do

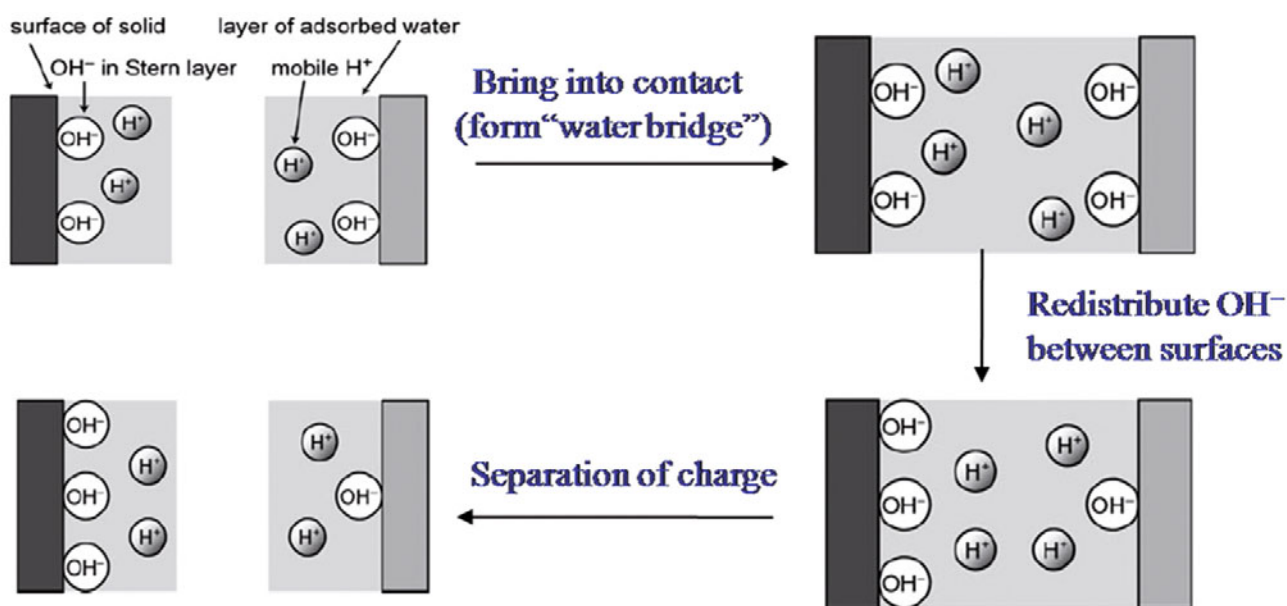


Fig. 4. Schematic view of the exchange of H^+ and OH^- ions during asymmetric collision (edited from L.S. McCarty and G.M. Whitesides [35]).

Table 2. Seven mechanisms recognised as potentially contributing to electric charges on sand particles.

| No. | Mechanism | Interpretation |
|-----|--|--|
| 1) | Cleavage/fractoelectrification | Charges are generated on sand particles as a result of cleavage or fracture. |
| 2) | Bombardment charging | Sand particles are charged due to solar wind bombardment or photoelectron ejection from sunlit surface. |
| 3) | Pyroelectrification | When a crystal is heated, electric charges will occur at the two ends of the crystal. |
| 4) | Piezolectrification | A crystal acquires charges when pressure is applied. |
| 5) | Polarisation by Earth's atmospheric electric field | Sand particles in the atmospheric electric field, as a kind of dielectric material, are polarised and the excess charges are repelled to the two sides of a sand particle. |
| 6) | Triboelectrification | Two neutral sand particles are charged by rubbing each other. |
| 7) | Contact electrification | Particles comprising of different materials contact each other and gain charges when they are separate. |

not transfer again. Lowell and Truscott [41] pointed out that the charged species are electrons, and the electrons trapped in high-energy states remain there for periods of days to centuries, which has been verified by phosphorescence and thermo-luminescence measurements [50, 51]. Except for electrons [19, 46, 48], the charged species can be generalised as ions (positive or negative) [52, 53] and holes [48].

It is worth noting that quite a few researchers have adopted the asymmetric contact charging model to explain the electrification and charge transfer of sand and

other insulating particles [18, 22, 44, 46, 48, 52, 53]. Kok and Lacks [46] deemed the charged species to be electrons and proposed a charging scheme for granular systems of identical insulators. Assuming that the initial densities of high-energy trapped surface states of particle i and j are both equal to ρ_H , then the number of electrons trapped in high-energy states tunneling from particle i to j is $N_H^i = \pi\rho_H e\delta_0 R_i(2R_j + \delta_0)/(R_i + R_j)$, where δ_0 is the tunneling distance and e is the elementary charge. After particle i and j separate, the net charge transfer Δq_i of particle i is $N_H^i - N_H^j$, that is, $\Delta q_i = \rho_H \pi e \delta_0^2 (R_i - R_j)/(R_i + R_j)$.

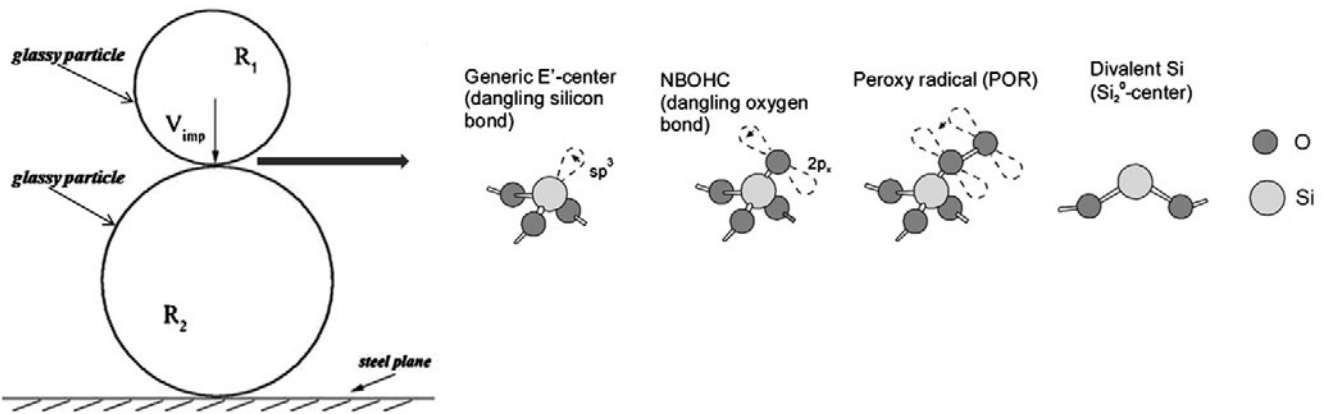


Fig. 5. Schematic view of asymmetric contact charging model, in which the charged species are holes formed by dangling bonds on the glassy particles' surfaces (SiO_2) (edited based on L. Skuja *et al.* [54]).

Therefore, when $R_i < R_j$, $\Delta q_i < 0$ which can explain why “larger particles tend to be positively charged and smaller particles tend to be negatively charged” [22]. Hu *et al.* [18] considered the grain-grain collisions as elastic solid contact processes described using the soft-sphere contact model, and demonstrated that the number of electrons trapped in the high-energy states tunneling from particle i to particle j is B_i times larger than the hard-sphere contact presented in Kok and Lack's work, and that the net transfer charge of particle i is $\Delta q_i = B_i N_{\text{H}}^i - B_j N_{\text{H}}^j$, where the coefficient B_i is related to the relative impact velocity, the relative impact angle and the particle size.

Furthermore, Hu *et al.* [48] suggested that the charged species should be holes for silica insulator such as sand grains, because the surface point defects in SiO_2 surfaces (*i.e.*, glass and quartz) are mostly electrons traps, also known as trapped-hole centres [54]. According to their experiments on contact charging of single collisions between glassy particles and a particle plane, the inversion of the density of high-energy trapped holes is in the range of $0.15 \div 0.6 \text{ nm}^{-2}$, and such a density corresponds to about $3.307\% \div 13.23\%$ of the total defects ($\sim 4.536 \text{ nm}^{-2}$ [54]) which is consistent with the assumption that the surface density of low-energy states is probably several orders of magnitude larger than that of the high-energy states [41, 46]. The contact charging model based on high-energy trapped holes transfer proposed by Hu *et al.* [48] can quantitatively predict the contact charging in a single collision as a function of the particle size and the impacting velocity, and can also explain the phenomenon that “larger particles tend to be positively charged and smaller particles tend to be negatively charged”. For Terrestrial and Martian land surfaces, SiO_2 is a dominant chemical species [55–58] and therefore holes can be regarded as the charge species of the electrification of wind-blown sand/dust systems on Earth or Mars. This includes wind-blown sand, sand/dust storms, dust devils, etc. [4, 5, 16]. Moreover, contact charging processes might be accompanied by mass transfer [59–61], since non-frictional contacts result in electron and/or ion exchange, while squeezing might produce mass transfer and bipolar charging [60]. Of

course, in non-frictional contacts rubbing could also lead to bipolar charging [62]. Therefore, further experiments are required to verify whether mass transfer takes place during the contact charging process between two sand particles.

3 The electric field of wind-blown sand and its prediction

A second important focus of research on the electrification of wind-blown sand is the E -field, which was inspired by several field observations and followed by the gradual development of theoretical prediction models. This section begins with a review of the history of the experimental apparatus developed to measure the E -field, followed by a discussion of recently observed results of E -fields in various dusty environments, such as wind-blown sands, dust storms, and dust devils. Finally a summary of theoretical studies to predict the E -fields in wind-blown sand flux will be given.

3.1 Field observations

In 1913, Rudge measured the E -fields in three types of weather conditions, *viz.* ordinary fine weather, a moderate dust storm, and a severe dust storm at Bloemfontein, with a radium-coated electrode electrometer. His recorded results showed that the E -field in a dust storm was upward pointing (opposite in direction to that in fine weather), and had a value of $5 \div 10 \text{ kV/m}$ [63]. In Rudge's experiments, an electrode was placed on the ground together with others that were mounted above the ground with certain wall-normal distances, and the E -fields were obtained by measuring the potential differences between pairs of electrodes. Demon *et al.* [64] first used the atmospheric electric field mill to measure E -fields during a severe dust storm in the north Sahara, Algeria. The observed E -fields were $\sim 15 \text{ kV/m}$ and downward in direction. The atmospheric electric field mill works by measuring the induced

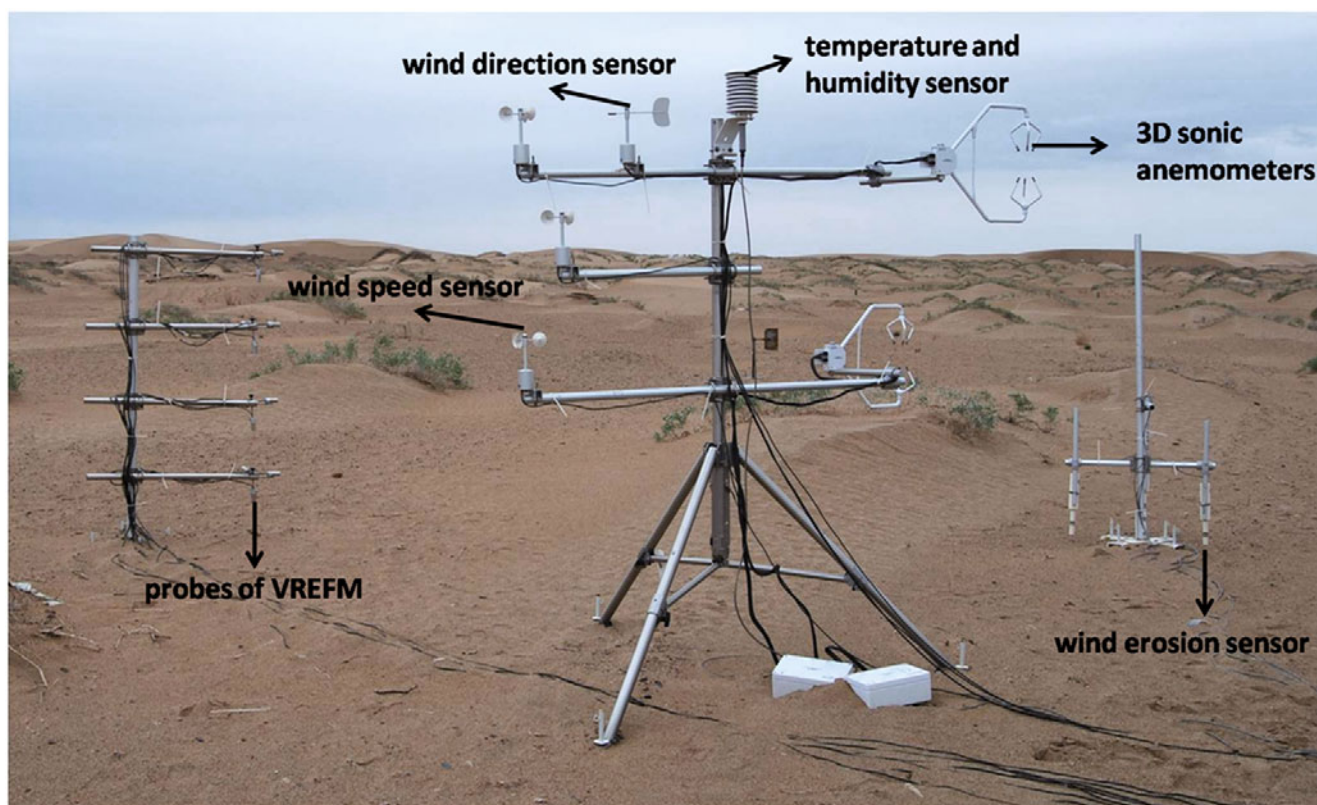


Fig. 6. The integrated field observation system which can give a synchronised measurement of three-dimensional wind velocities, three-dimensional E -fields, temperature, humidity, wind-blown sand transport intensity, and dust concentration.

charge, *i.e.*, first the conductive blade (also called the stator) which is exposed to air flow generates induced charges due to the atmospheric electric field, and then a motor within the probe twirls the other earth shield blades (also called rotors) which alternatively sense the induced charges on the stator and produce alternating signals. Finally, the electric field intensity along with the direction of the stator can be obtained by converting the alternating signals with a data collection system. Following this, the two kinds of experimental apparatus were widely adopted by many researchers to measure the E -fields in dusty environments [4, 5, 15, 25, 28, 65–71]. However, both kinds of apparatus are inevitably affected by the impact of saltating particles on the probe. Further, the accuracy of the atmospheric electric field mill is associated with the area of the sensor and the rotor's speed, but a large sensor area (with a diameter of around 8 cm) may disturb the real E -field. Johnston *et al.* [72] and Renno *et al.* [73] designed an improved atmospheric electric field mill where the diameter had been reduced to 2 cm. However, the influence of saltating particles still exists, which results in the rotor's speed deviating by 30% from the standard speed, and thus affecting the accuracy. For the radium-coated electrode electrometer, it can only give an average value within a certain range of heights. After a series of tests, the author's group found that when applying an external E -field along directions distinct from the direction of probes or two electrodes' connection, we can obtain mea-

sured values that deviate significantly from the real values. This means that an E -field can only be accurately measured when the probes are aligned in the direction of the E -field.

Recently, the author's group designed a vibrating-reed mill for measuring the E -fields in wind-blown sands whose sensor has a diameter of about 2 cm. The measuring principle is based on the dynamic capacity, *i.e.*, two parallel metallic plates constitute a capacitor, where the inner polar plate is hidden inside the probe and can vibrate (driven by a motor) and the outer polar plate is fixed as a probe surface to produce induced charges. A rounded shielding case is mounted on the top of the probe so as to prevent the influence of E -fields from the others directions. When the motor-driven plate vibrates, the distance between the two plates changes periodically and generates a periodic charge-discharge. Finally, the E -fields can be calculated via a current signal processing system. Tests show that the shielding case on top of the probe can attenuate the influence of E -fields from other directions by 90%, and when calibrating the effect of the shielding case the induction sensitivity of the outer polar plate should be considered. With the new electric field mill, we can achieve measurements of one- and even three-dimensional E -fields.

Integrating the vibrating-reed electric field mill (VREFM) into the wind erosion measurement system (designed by the United States Department of Agricul-

Table 3. The measured results of E -fields in different dusty environments.

| Reference | Dusty environment | Height (m) | E -field intensity (kV/m) | Direction |
|-----------------------------|-------------------|------------|-----------------------------|---------------------|
| Rudge [63] | Dust storm | 0.2 | $5 \div 10$ | Upward |
| Demon <i>et al.</i> [64] | Dust storm | 0 | 15 | Downward |
| Harris [65] | Dust storm | 0 | 5 | Upward |
| Kamra [26] | Dust storm | 1 | 5 | Upward and Downward |
| Zhang <i>et al.</i> [31] | Dust storm | 16 | 200 | Upward |
| Williams <i>et al.</i> [71] | Dust storm | 0 | 8 | Upward and Downward |
| Freier [4] | Dust devil | 0 | 0.6 kv/m | Upward |
| Farrell <i>et al.</i> [70] | Dust devil | 0 | 10 | Upward |
| Schmidt <i>et al.</i> [5] | Wind-blown sand | 0.017–2 | $+166 \div -0.18$ | Upward |

ture Wind Erosion and Water Conservation Unit), we can make synchronised measurements of multi-sites, three-dimensional wind velocities, three-dimensional E -fields, temperature, humidity, wind-blown sand transport intensity, and dust concentration. Figure 6 shows the integrated measurement system, where the sampling frequency is 10 Hz for the three-dimensional ultrasonic anemometer, and 1 Hz for the other apparatus.

For the E -field intensity, it has been generally accepted that the E -field generated by wind-blown sand is much larger than the fair weather atmospheric electric field. For instance, measurements on a sand dune [5] showed that the E -field was upward in direction and as large as 166 kV m^{-1} at a height of 0.017 m for a mean wind speed of 12 ms^{-1} (at a height of 1.5 m). So far, numerous E -field measurements have been made in dusty environments, as listed in table 3. In general, the strongest E -fields are in dust storms, then dust devils and wind-blown sand flows. This is mainly due to the differential space distributions of dust concentrations in the three kinds of dusty environments. Other factors, such as surface temperature, etc., also have an important influence on the measured E -fields [65,66]. In wind-tunnels, more accurate measurements of the E -fields generated by wind-blown sands can be obtained [15]. For example, Zheng *et al.* found that for both “uniform” and mixed sands, the magnitude of the E -field increases gradually as the height increases (as observed in field observations [5]), and also increases as the wind velocity increases. At the same wind velocity, the smaller the sand particle’s size is, the larger the E -field becomes. These results agree with the percentage profile of small sand particles which also increases with the height and wind velocity and, as explained above, small sand particles have relatively high charge-to-mass ratios [15]. Meanwhile, the E -fields of mixed sands are much larger than “uniform” sands. For a wind speed of 20 m/s, the maximum value of the former is at least 20 times higher than the latter [15], because the charge-to-mass ratio of mixed sands is much larger than “uniform” sands. Furthermore, Zheng *et al.* [15] presented an opinion that the E -field in wind-blown sands is mainly generated by saltat-

ing particles, whereas Schmidt *et al.* [5] concluded that the E -field is mainly generated by creeping particles.

For the directions of E -fields, Freier [4] noted that the E -field during dust devils in the Sahara Desert is upward-pointing and much stronger than the fair weather atmospheric field, though several researchers found that both upward- and downward-pointing E -fields can be observed in dust storms and their magnitude can reach up to several kV/m [26,71]. Schmidt *et al.* [5] and Zheng *et al.* [15] separately but almost simultaneously made systematic electric-field measurements in wind-blown sand flux with the atmospheric electric field mill, where the former were carried out in the field and the latter were carried out in a wind-tunnel. Both results suggested that the E -fields in wind-blown sand flux are upward-pointing. Now it is generally accepted [8] that the electric field in wind-blown sand is upward-pointing [4,5,16,31,65–70] since the small particles saltating in air are usually negatively charged, while the large particles creeping on the bed surface are positively charged (for dust devils, small particles are easier to move away from the centre of dust devils than large particles). Using the apparatus shown in fig. 6, the author’s group recently observed a dust storm lasting 23 hours from its formation to its decaying stage, and found that there exist both vertical and horizontal E -fields in dust storms. Figure 7 shows the measured E -fields (0.8 m) together with wind speed (0.8 m), temperature (2 m) and wind-blown sand flux (0.1 m). During the dust storm, the horizontal E -field, which reached up to 200 kV/m, was larger than the vertical E -field and up-wind pointing.

Obviously, it is not reasonable to explain the generation of horizontal E -fields in wind-blown sand flux with the same mechanism as vertical E -fields, which we will discuss later. From fig. 7 we can see that at the developing and decaying stages of the dust storm, the streamwise wind velocity is an important factor affecting vertical and horizontal E -fields. Of course, the relationships between E -fields and wind velocity, temperature, humidity, dust concentration, as well as wind-blown sand transport intensity are very complicated and deserve further study.

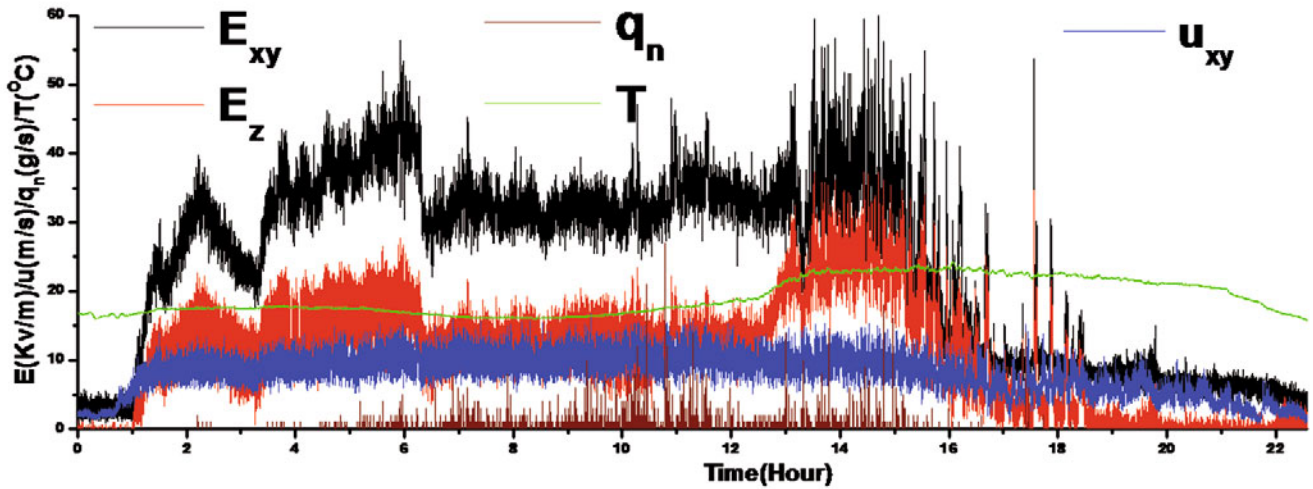


Fig. 7. The variation of the E -field (0.8 m), wind speed (0.8 m), temperature (2 m) and wind-blown sand flux (0.1 m) with time of a dust storm passing through Minqin, China on April 20, 2011, the duration of which was about 23 hours (E_{xy} and E_z are the streamwise and vertical E -fields, respectively, u_{xy} is the streamwise wind velocity, q_n is the wind-blown sand flux, and T is temperature).

3.2 Theoretical predictions

As one of the earliest theoretical studies, Zheng *et al.* [74] reduced the E -field generated by wind-blown sands to a one-dimensional problem by assuming a steady state of the wind-blown sand flow and that the mass flux or saltating particles concentration was constant in the streamwise (x) direction, in other words, the saltating sand concentration is uniform in the x -direction. In their simulations, the E -field of a point charge was quantified by Coulomb's law, and the average charge-to-mass ratio of the saltating particles was assumed to be the same as that found by Schmidt *et al.* [5]. Their results showed that the total E -field close to the bed surface could reach up to several hundreds of kilovolts per meter in magnitude, and decreased quickly with increasing height. Moreover, the variation of the E -field with height was not monotonic: when the direction of the E -field changed from upward (opposite to the fair-weather electric field) to downward (same as the fair-weather electric field), the E -field intensity increased from zero to several kilovolts per meter in magnitude and then decreased to that of fair weather. In addition, the sign of the charges acquired by the particles, the charge-to-mass ratios of the particles, the wind velocity and the sand particles' transport type all had obvious influences on the E -field. The profile of the E -field induced by saltating particles was different from that induced by creeping particles. The E -field intensity increased with increasing wind velocity and increasing charge-to-mass ratio of the charged sand particles. Based on the model of Zheng *et al.* [74], Kok and Renno [16] developed a physical model by considering the charge transfer during particle collisions and pointed out that i) the existence of electrostatic forces enhanced the concentration of saltating particles, and ii) the downward electrostatic forces had a pronounced effect on the lower saltating particles' trajectories, thus reconciling the difference between numerical

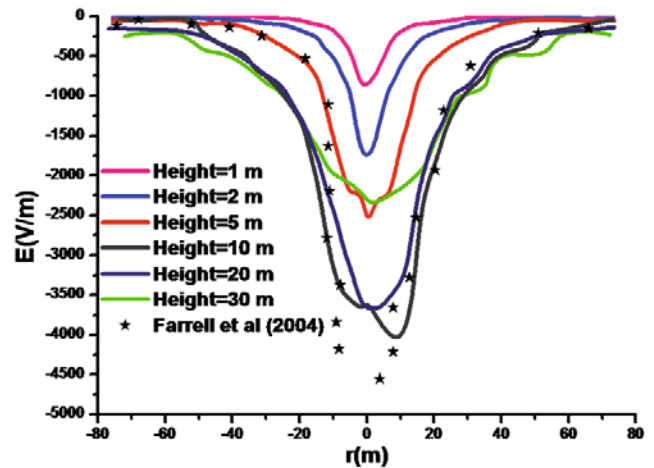


Fig. 8. The E -field at various heights in a dust devil when it tends to be stabilised [75].

models and measurements. In a similar manner, Huang *et al.* [75] modeled the E -fields in dust devils, as shown in fig. 8, and the modeled results are in good agreement with measurements by Farrell *et al.* [68] in the Arizona desert.

It should be noted that wind-tunnel experiments by Shao and Raupach [76] indicated that there exists an "overshoot" phenomenon in the evolution of wind-blown sand flux, that is, as the streamwise distance increases, the mass flux first rapidly increases to a maximum, and then decreases to an equilibrium value. This implies that the saltating mass flux or particle concentration is non-uniform, at least during the development stage of wind-blown sand flux. Such a phenomenon is also confirmed by numerous field and wind-tunnel measurements [76–81]. By considering the streamwise spatial variation of the sand concentration during the evolution

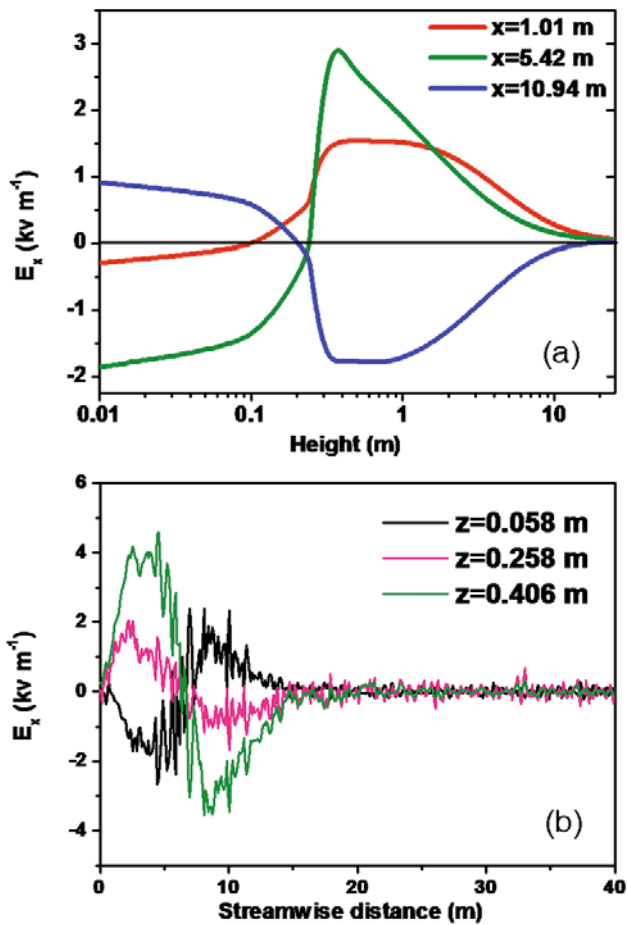


Fig. 9. The horizontal component of the E -field in wind-blown sand flux. (a) Height profile of the horizontal E -field. (b) Horizontal E -field varying with streamwise distance, where the friction velocity $u_* = 0.5 \text{ m s}^{-1}$, and sand grain diameter $D = 0.25 \text{ mm}$.

of wind-blown sand flux, Zhang *et al.* [82] made theoretical predictions concerning the E -fields of wind-blown sand. Their results showed that the horizontal E -field could reach up to several kilovolts per metre and that the spatial variation of the particle concentration played an important role in the generation of the horizontal E -field. Figure 9 displays three distinct layers of the horizontal E -field: near the sand surface the horizontal E -field is upwind and its magnitude gradually reduces with height from several V/m to zero; then its direction reverses and its magnitude increases with height to a maximum value; and eventually it decreases with height to zero at around 3 m. Moreover, a similar “overshoot” of the horizontal E -field can be identified, that is, the horizontal E -field first increases and then decreases with streamwise distance, with a peak value at $L/2$ (L is the saturation length of the wind-blown sand flux).

In summary, existing facilities and theoretical models have helped to improve our understanding of the E -fields in wind-blown sand flux. However, three-dimensional fine measurements in the field are still inadequate, and further efforts are required to conduct systematic measurements

and quantitative predictions so as to draw a clearer picture of the spatio-temporal characteristics of the E -fields in natural granular disasters, especially the streamwise E -field and the relationship between E -fields and other factors.

4 Influence of E -fields produced by charged sands

In strong sand storms, E -fields produced by charged sand particles could potentially lead to many failures, such as electric spark, electric corona and point discharge of measuring instruments [21], flashover and breakdown of high-voltage transmission lines, etc. [10]. In this section we focus on the effect of the E -fields on wind-blown sand flux and quantitative analysis of the influence of wind-blown sand flux on the propagation of wireless communication signals.

4.1 On the development of wind-blown sand flux

It is well known that in wind-blown sand flux the wind moves the sand particles in one, or a combination, of three ways: creep or reptation, saltation and suspension [83, 84]. Except for dust storms in which a relatively high proportion of particles move in suspension, saltation plays the dominant role in wind-blown sand flux near surfaces [85], therefore most quantitative simulations of wind-blown sand flux focus on modeling sand saltation in air flows [85–88]. However, there have been a few attempts to incorporate the effect of charges. Owing to the difficulty of direct measurement, answers to this question have been limited to conjectures for a long period. For example, Greeley and Iversen [89] inferred that charges of sand particles and the E -field in wind-blown sand flux may have an effect on the initiation of sand lifting and the trajectories of saltating sand particles. At the same time, they suggested that the effect on the wind-blown sand movements on other planets (such as Mars, Saturn, etc.) may be more remarkable than on Earth.

It was not until 1998 that Schmidt *et al.* [5] made the first measurements of the average charge-to-mass ratios and E -fields during a wind gust, and calculated the effect of electrostatic forces on saltation trajectories. These measurements indicated that the trajectory lengths were increased by 63% and reduced by 43%, respectively, for positively and negatively charged particles when compared with particles without charge moving in the E -field, and the corresponding trajectory heights were increased by 67% and reduced by 46%, respectively. Schmidt *et al.*'s calculations did not account for the nonlinear coupling interaction between sand saltation and the wind, however, and both experiment and theory [8, 83, 90, 91] have shown that the counteractive effect from saltating sand particles to air flows, *i.e.*, the negative feedback mechanism [8], cannot be neglected.

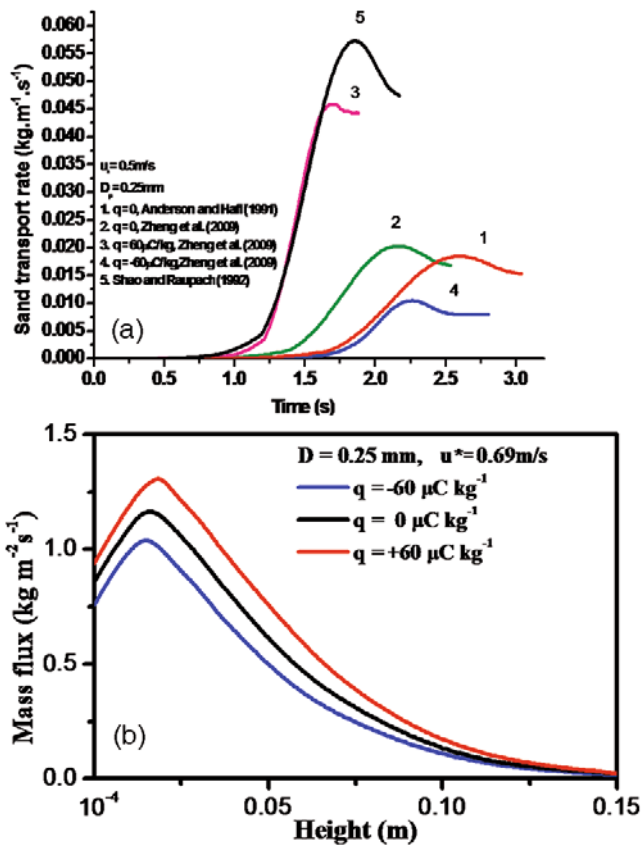


Fig. 10. (a) Simulated and measured sand transport rate versus time; (b) mass flux profile versus height (q is the charge-to-mass ratio).

The author’s group proposed a statistic-coupling model [8] to achieve quantitative simulations of the formation and evolution of windblown sand flux wherein the nonlinear coupling effects due to wind field, sand motion, E -field and thermal diffusion were incorporated. With this model Yue and Zheng [92] found that: for saltating particles with positive charges, the time required for the wind-blown sand flux to reach its steady state (saturation time) was shortened by 21%, while for saltating particles with negative charges the corresponding required time was prolonged by 6%, as shown in fig. 10a. When sand particles are assumed to be positively charged, the simulated results of Yue and Zheng [92] are in good agreement with the experimental results obtained by Shao and Raupach [76], with the differences for the saturation time and the sand transport rate being only 7.4% and 8%, respectively. Comparisons between the results given by the stochastic-coupling model and Schmidt *et al.*’s calculations showed that the latter overestimated the effect of electrostatic forces on saltation trajectory lengths, but underestimated the effect on trajectory heights. Zheng *et al.* [93] also found that the vertical profile of windblown sand flux displayed not a simple negative-exponential decline but rather a stratification pattern, *i.e.*, close to the ground surface the mass flux first increased linearly with height, then tended to a saturation state and reached a

maximum value, and finally followed an exponential decline, as shown in fig. 10b. Such a stratification profile provides a theoretical explanation of the phenomenon where the most severely damaged parts of plants or buildings standing in wind-blown sand flux are not at the root, but at certain heights from the ground.

Following the work of Zheng *et al.* [15,74], Kok and Renno [16] and Hu *et al.* [18] incorporated charge transfer between sand particles during particle/bed collisions into their models, and investigated the effect of charged sands and E -fields on sand transport in wind-blown sand flux. Kok and Renno [94] applied an external E -field on a sand bed by placing two electrode plates above and below the bed, and found that when the E -field exceeded 80 kV/m the threshold shear velocity for sand entrainment was obviously reduced. Furthermore, they concluded that E -fields during wind-blown sand transport could enhance the erosion of soil particles, and increase the particle concentration at a given wind shear velocity. Rasmussen *et al.* [95] also noted that sand transport was obviously enhanced when the E -fields were 160-280 kV/m. Pähtz *et al.* [96] explained the charging of sand particles by the polarisation effect due to external E -fields, *i.e.*, when two initially electrically neutral particles collide with each other, the pre-existing electric field results in the two particles being repolarised with additional unit charges, therefore providing a charge transfer mechanism for identical insulators within a strong E -field. However, in natural wind-blown sand flux the fair weather atmospheric electric field cannot provide such a high E -field (several tens of kilovolts per metre) for the initial polarisation of sand particles. The interaction between wind-blown sand transport and E -fields can be regarded as the following process. Initially particles on the sand surface start creeping under the act of wind force, and squeezing and rubbing lead to charge transfer between sand particles which forms an initial E -field. This initial E -field then promotes sand lifting, and enhances the concentration of charged sand particles. Meanwhile, the E -field generated by saltating sand particles is strengthened. Due to the negative feedback effect of saltating sand particles on air flows, the wind velocity is gradually reduced until it approaches a steady state. In other words, the positive feedback effect of charged sand particles strengthens the wind-blown sand transport and E -fields, while the negative feedback effect of saltating particles leads to a steady or saturation state of wind-blown sand flux.

It should be noted that all of the above studies have neglected the existence of streamwise E -fields. The author’s group attempted to add a streamwise E -field term into the model of wind-blown sand flux by considering the interaction between saltating sand particles and air flows, and the results showed that, when compared with vertical E -fields, streamwise E -fields also played important roles in wind-blown sand flux. For example, they can reduce the mass flux and shorten the time taken for wind-blown sand flux to reach its steady state, as shown in fig. 11. This is because the streamwise E -fields exert a force on the sand particles that oppose the wind and therefore reduces the

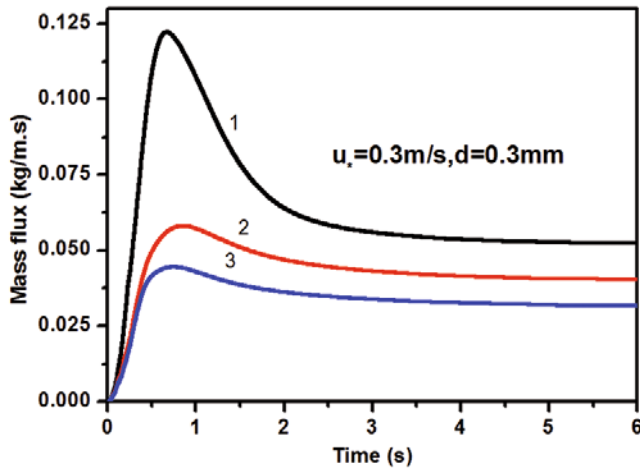


Fig. 11. Effect of E -fields on the mass flux of wind-blown sand transport, in which curve 1 (black) represents simulated results without considering the effect of streamwise or vertical E -fields, curve 2 (red) represents results that incorporate the effect of vertical E -fields but not streamwise E -fields, and curve 3 (blue) represents results that consider both streamwise and vertical E -fields.

streamwise velocities of the sand particles, thus lowering the mass flux. Of course, quantitative explanations require detailed analysis of the effect of streamwise E -fields on the distribution of impacting velocities, particle/bed collisions and the initiation of sand transport.

4.2 On the attenuation of electromagnetic waves

Another noteworthy issue arising from the influence of electrification of wind-blown sand is the attenuation of electromagnetic waves. In 1983, Haddad *et al.* [97] found that when electromagnetic waves of 9.4 GHz propagate through a dust storm with mass density $6 \times 10^{-5} \text{ gm/m}^3$, the attenuation is 0.034 dB/m. Meanwhile traditional scattering theories estimated an attenuation of 0.1 dB/km [97], which is about 30 times higher than the measured value. This large discrepancy between experimental results and theoretical estimates was not reconciled until 2005, when Zhou *et al.* [30] put forward a new theoretical approach in which it was assumed that the electric charge of a sand particle is distributed partially on the sand surface. Their results also indicated that when considering the effect of charged sand particles on attenuation, parameters including polarity, surface charge density and electric charge distribution area were all important for the calculation of the attenuation coefficient based on the Rayleigh approximation, as shown in fig. 12. Further studies found that: when sand particles acquire electric charges, the Rayleigh approximation is no longer valid [98]. A possible means of resolving this problem is the generalized Mie scattering theory, based on which the extinction efficiency of a granular system with partially distributed charges can be derived. An implication from this theoretical scheme is that the effect of sand particles with partially distributed charges is more important

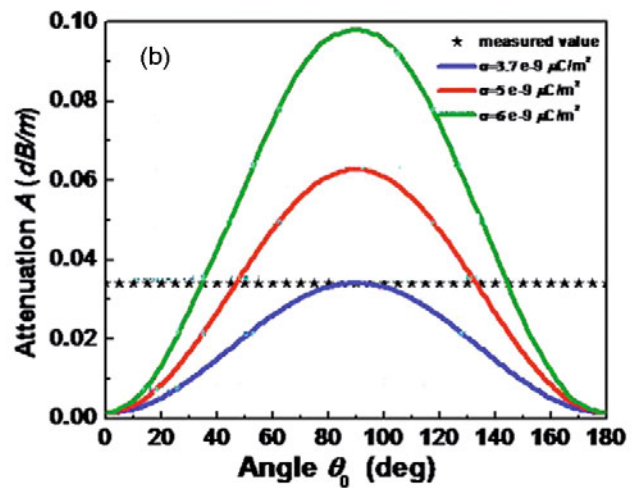
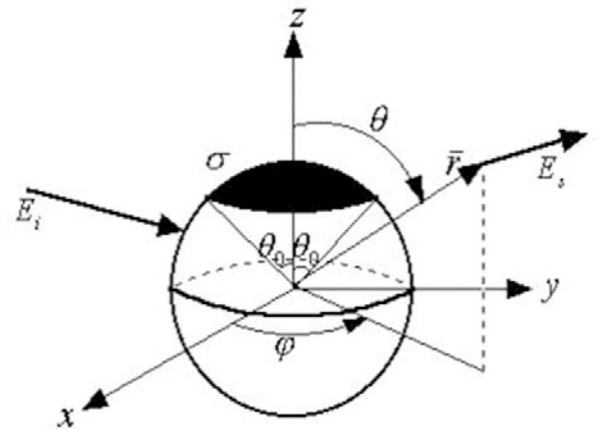


Fig. 12. (a) Schematic view of a sand particle with the electric charge distributed on a spherical cap (indicated by the black domain) with angle θ_0 and density of surface charge σ , E_i and E_s represent the incident and scattering electromagnetic wave penetrating in the spherical sand particle, respectively. (b) Characteristic curves of the attenuation coefficient varying with angle θ_0 of electric charge distribution for different densities of surface charges σ . Measured value: attenuation coefficient $A = 0.034 \text{ dB/m}$ [30].

than the multiple scattering effect among sand particles for dust storms with visibility larger than 1 m, though the latter effect might increase with the sand concentration of dust storms.

The influence of charged sand/dust particles on the propagation of electromagnetic waves poses a problem for the accuracy of satellite remote sensing, which is known to be affected by dust storms. Until now, the spatial-temporal distribution of dust storms has been surveyed using the information extracted from remote sensing data [99]. For example, AMSR-E is used to monitor the radiation energy of a dust storm in terms of brightness temperature through 6 bands of microwaves with 12 channels [100], in which the difference between the horizontal and vertical polarised brightness temperatures is a key pa-

parameter used to judge the existence of dust storms [101], and to further identify the dust concentration [102]. However, the calculated brightness temperature [103] is about 10 K higher than the value given by remote sensing data, moreover, the brightness temperature of dusty weather is larger than that of fair weather, which is the reverse of the result of remote sensing data. The author's group investigated this issue and attributed the attenuation of electromagnetic waves to dust charges which nonlinearly decreased with the frequency of the electromagnetic waves. This implies that the attenuation is most pronounced for electromagnetic waves with low frequencies, for example below 10 GHz. Note that for electromagnetic waves with high frequencies, for example above 100 GHz, especially for optical frequency electromagnetic waves, the effect of sand charges can be ignored [104]. Therefore the reason for the discrepancy between the calculated results of Ge *et al.* [103] and the measured data can be attributed to the low-frequency electromagnetic waves used in the calculations. More precisely, the calculation scheme, which assumes the calculated radiation brightness temperature is equal to the remote sensing data for 6.9 GHz electromagnetic waves, overestimates the number of dust particles, which results in the calculated radiation brightness temperature being higher than the remote sensing data when using 89 GHz electromagnetic waves.

Whether considered in terms of the aspect of wind-blown sand flux or the propagation of electromagnetic waves, the E -fields produced by charged sand particles play a significant role that directly influences our predictions and related applications. Therefore, identification and quantitative predictions of the influence become a fundamental task when dealing with dusty or granular cases.

5 Issues for future research

Many important studies have been carried out in the field of electrification of wind-blown sand and notable advances have been achieved, particularly in exploring the charging mechanism of sand particles, and investigating the laws and influence of the E -field produced by charged sands. However, many challenges remain in experimental techniques (either in field or wind-tunnel measurements), mechanism analysis, quantitative prediction, and numerical simulations.

5.1 Experimental techniques

For experimental techniques, it is necessary to develop an integrated non-contact measurement system which can not only perform a real-time and synchronous measurement of electric charges, charge-to-mass ratios of sand particles and the direction and intensity of 3D E -fields but also provide simultaneous information pertaining to the wind velocity, temperature, humidity, particle size distribution, spatio-temporal even land surface conditions, etc. As for the necessity of non-contact design, it is propelled

by the fact that experimental instruments have considerable influence on the motions of sand/dust particles with micron scales, and therefore reduce the accuracy of measurements. In addition, the impact of moving particles also affects instrument sensitivity, and can even cause failure. New measuring principles (experimental methods) might be required to resolve this difficulty. Furthermore, enhancing sampling frequency and accuracy as well as ensuring synchronisation can provide a better understanding of the mechanisms of sand particles' charging and the formation of E -fields, as well as the changing laws of the electrification of wind-blown sand. For example, the number of charges and polarity acquired by sand particles, the intensity and direction of E -fields and their spatial distribution features, as well as key factors affecting these quantities.

5.2 Quantitative analysis

For quantitative analysis, the primary task is to establish a 3D model with respect to the coupling effect between wind field, sand motion, E -field and thermal diffusion, so that a comprehensive understanding of the E -field in wind-blown sand flux, especially revealing the 3D changing law of E -fields during dust storms, and quantification of the impact of E -fields on sand/dust transportation could be achieved. Notably, besides the interaction between wind fields and sand motions, there is another strong interaction effect between sand charges, E -fields and sand transport intensity which could not be neglected when modeling wind-blown sand flux. Therefore, a key requirement in practice when predicting the 3D E -fields in wind-blown sand flux is to establish a multi- or trans-scales numerical scheme with respect to this multi-physics coupling effect. In addition, analysis on the effect of charged sand particles on the scattering of electromagnetic wave and the attenuation of microwave propagation suggest a need to incorporate the effect of i) moving sand/dust media introduced by its spatial random distribution, ii) the variation of electric charges during the evolution of wind-blown sand/dust flux which might produce oscillation current under the excitation of electromagnetic wave and iii) the rationality of analytical models such as the applicability of the Mie theory and the corresponding boundary conditions.

5.3 More challenging issues

Another important issue that needs to be addressed is how to identify and utilise the influence of the electrification of wind-blown sand. For the former, in addition to the effect of charged sand particles on wind-blown sand/dust flux, another important issue that has not yet attracted enough attentions is the calibration of equipment used in dusty environments, such as PIV, PDA, satellite remote sensing, atmospheric temperature profiler, boundary layer wind-profile radar, etc. All this equipment is based on direct measurements or indirect inversions from electromagnetic-wave scattering signals, which may include additional information due to the effect of charged sand particles.

Therefore, it is quite necessary to effectively identify the effect of electric charges and make suitable calibration adjustments when analysing the measured data. For the latter, the effect of charged sands can be positively utilised to retrieve some not-so-easily or accurately measured quantities in harsh experimental conditions, such as the dust concentration profile during a dust storm. Indeed, more efforts are required to understand the negative and positive effect of the electrification of wind-blown sand, even to exploit a possible way to transform the power of strong E -fields in wind-blown sand flux into available energy.

This research was supported by a grant from the National Natural Science Foundation of China (Nos. 11232006, 11072097 and 11121202), the Science Foundation of Ministry of Education of China (No.308022), Fundamental Research Funds for the Central Universities (lzujbky-2009-k01) and The National Key Technology R&D Program (No.2013BAC07B01). The author expresses her sincere appreciation for these financial supports.

References

1. E.W.B. Gill, *Nature* **18**, 2 (1948).
2. D.S. Schmidt, R.A. Schmidt, J.D. Dent, *Boundary-Layer Meteorol.* **93**, 29 (1999).
3. T. Mather, R. Harrison, *Surv. Geophys.* **27**, 387 (2006).
4. G.D. Freier, *J. Geophys. Res.* **65**, 3504 (1960).
5. D.S. Schmidt, R.A. Schmidt, J.D. Dent, *J. Geophys. Res.* **103**, 8997 (1998).
6. M. Gordon, P. Taylor, *Boundary-Layer Meteorol.* **130**, 97 (2009).
7. T. Miura, T. Koyaguchi, Y. Tanaka, *Bull. Volcanol.* **64**, 75 (2002).
8. M.M. Awad, H.M. Said, B.A. Arafa, A.E. Sadeek, *CIGRÉ*, 2002 Paper No. 15-306, 1 (2002).
9. Y.-H. Zhou, Q. Shu He, X. Jing Zheng, *Eur. Phys. J. E* **17**, 181 (2005).
10. Helicopter Static-Electricity Phenomenon, <http://www.defence.pk/forums/air-warfare/75190-helicopter-static-electricity-phenomenon.html>.
11. Electric Dust Devils, <http://www.holoscience.com/wp/electric-dust-devils/>.
12. W.M. Farrell, G.T. Delory, S.A. Cummer, J.R. Marshall, *Geophys. Res. Lett.* **30**, 2050 (2003).
13. Iceland Volcano Pictures: Lightning Adds Flash to Ash, http://news.nationalgeographic.com/news/2010/04/photogalleries/100419-iceland-volcano-lightning-ash-pictures/#/iceland-volcano-lightning-5.1911_600x450.jpg.
14. When all hell breaks loose: Lightning tears the sky apart above the glow of the Chilean volcano, <http://www.dailymail.co.uk/news/article-1394503/Chile-volcano-causes-ash-cloud-lightning-tears-sky-apart.html>.
15. X.J. Zheng, N. Huang, Y.-H. Zhou, *J. Geophys. Res. D* **108**, 4322 (2003).
16. J.F. Kok, N.O. Renno, *Phys. Rev. Lett.* **100**, 014501 (2008).
17. X.J. Zheng, *Mechanics of Wind-blown Sand Movements* (Springer, Berlin, 2009).
18. W. Hu, L. Xie, X.J. Zheng, *Eur. Phys. J. E* **35**, 22 (2012).
19. C.E.S. Phillips, *Proc. R. Inst. G. B.* **19**, 742 (1910).
20. W.A.D. Rudge, *Proc. R. Soc. London, Ser. A* **90**, 256 (1914).
21. R. Greeley, R. Leach, *Rep. Planet. Geol. Program, 1977-1978, NASA TM 79729*, 236 (1978).
22. K.M. Forward, D.J. Lacks, R.M. Sankaran, *Geophys. Res. Lett.* **36**, L13201 (2009).
23. J. Latham, C.D. Stow, *Q. J. R. Meteorol. Soc.* **94**, 415 (1968).
24. E.J. Workman, S.E. Reynolds, *Phys. Rev.* **78**, 254 (1950).
25. S. Fuerstenau, G. Wilson, *Inst. Phys. Conf. Ser.* **178**, 143 (2004).
26. A.K. Kamra, *J. Geophys. Res.* **77**, 5856 (1972).
27. J. Latham, *Q. J. R. Meteorol. Soc.* **90**, 91 (1964).
28. K.M. Forward, D.J. Lacks, R.M. Sankaran, *Phys. Rev. Lett.* **102**, 028001 (2009).
29. J.J. Qu, M. Yan, G. Dong, H. Zhang, R. Zu, W. Tuo, A. Zhao, Z. Xiao, F. Li, B. Yang, *Sci. China Ser. D-Earth Sci.* **47**, 529 (2004).
30. Y.-H. Zhou, Q. Shu He, X. Jing Zheng, *Eur. Phys. J. E* **17**, 181 (2005).
31. H.F.W. Zhang, Tao Qu, Jian Jun Yan, Mu Hong, *Chin. J. Geophys.* **47**, 47 (2004).
32. P.S.H. Henry, *Br. J. Appl. Phys.* **4**, S31 (1953).
33. M.D. Hogue, C.R. Buhler, C.I. Calle, T. Matsuyama, W. Luo, E.E. Groop, *J. Electrostat.* **61**, 259 (2004).
34. M.D. Hogue, E.R. Mucciolo, C.I. Calle, C.R. Buhler, *J. Electrostat.* **63**, 179 (2005).
35. L.S. McCarty, G.M. Whitesides, *Angew. Chem. Int. Ed.* **47**, 2188 (2008).
36. S.P. Kanagy, C.J. Mann, *Earth-Sci. Rev.* **36**, 181 (1994).
37. C.D. Hendricks, *Electrostatics and Its Applications*, edited by A.D. Moore (Wiley, New York, 1973) pp. 57-85.
38. A.T. Szaynok, W. Wolniewicz, *J. Electrostat.* **1**, 381 (1975).
39. I.B. Cadoff, E. Miller, *Thermoelectric Materials and Devices* (Reinhold Publishing Corporation, New York, 1960).
40. J.W. Peterson, *Phys. Rev.* **76**, 1882 (1949).
41. J. Lowell, W.S. Truscott, *J. Phys. D-Appl. Phys.* **19**, 1281 (1986).
42. J. Lowell, W.S. Truscott, *J. Phys. D-Appl. Phys.* **19**, 1273 (1986).
43. J. Lowell, A.C. Rose-Innes, *Adv. Phys.* **29**, 947 (1980).
44. D.J. Lacks, A. Levandovsky, *J. Electrostat.* **65**, 107 (2007).
45. T. Shinbrot, H.J. Herrmann, *Nature* **451**, 773 (2008).
46. J.F. Kok, D.J. Lacks, *Phys. Rev. E* **79**, 051304 (2009).
47. J.L. Daniel, R.M. Sankaran, *J. Phys. D-Appl. Phys.* **44**, 453001 (2011).
48. W. Hu, L. Xie, X. Zheng, *Appl. Phys. Lett.* **101**, 114107 (2012).
49. S.J. Desch, J.N. Cuzzi, *Icarus* **143**, 87 (2000).
50. J.T. Randall, M.H.F. Wilkins, *Proc. R. Soc. London, Ser. A* **184**, 390 (1945).
51. A. Kron, T. Reitberger, B. Stenberg, *Polym. Int.* **42**, 131 (1997).
52. R. Pham, R.C. Virnelson, R.M. Sankaran, D.J. Lacks, *J. Electrostat.* **69**, 456 (2011).
53. G.S.P. Castle, *Proc. ESA Annual Meeting on Electrostatics*, Paper M1 (2008).

54. L. Skuja, M. Hirano, H. Hosono, K. Kajihara, *Phys. Status Solidi C* **2**, 15 (2005).
55. J. Du, A.N. Cormack, *J. Am. Ceram. Soc.* **88**, 2532 (2005).
56. S. Sharif, *IEEE Trans. Geosci. Remote Sensing* **33**, 353 (1995).
57. F.B. Gross, S.B. Grek, C.I. Calle, R.U. Lee, *J. Electrostat.* **53**, 257 (2001).
58. J.R. Green, J.D. Nelson, H.A. Perko, *Space 2002 and Robotics* (The American Society of Civil Engineers, Reston, 2002), pp. 176-189.
59. M.W. Williams, *IEEE Trans. Ind. Appl.* **47**, 1093 (2011).
60. H.T. Baytekin, B. Baytekin, J.T. Incorvati, B.A. Grzybowski, *Angew. Chem. Int. Ed.* **51**, 4843 (2012).
61. M.W. Williams, *J. Electrostat.* **70**, 233 (2012).
62. N. Knorr, *AIP Advances* **1**, 022119 (2011).
63. W.A.D. Rudge, *Nature* **91**, 31 (1913).
64. L. Demon, P. DeFelice, H. Gondet, Y. Kast, L. Pontier, *J. Rech. Cent. Natl Rech. Sci.* **24**, 126 (1953).
65. D.J. Harris, *Nature* **214**, 585 (1967).
66. D.J. Harris, *Planetary Electrodynamics*, edited by S.C. Coroniti, J. Hughes, Vol. 1 (Gordon and Breach, New York, 1969) pp. 39-47.
67. C.D. Stow, *Weather* **24**, 134 (1969).
68. W.M. Farrell, P.H. Smith, G.T. Delory, G.B. Hillard, J.R. Marshall, D. Catling, M. Hecht, D.M. Tratt, N. Renno, M.D. Desch, S.A. Cummer, J.G. Houser, B. Johnson, *J. Geophys. Res.* **109**, E03004 (2004).
69. N.O. Renno, V.J. Abreu, J. Koch, P.H. Smith, O.K. Hartogensis, H.A.R. De Bruin, D. Burose, G.T. Delory, W.M. Farrell, C.J. Watts, J. Garatza, M. Parker, A. Carswell, *J. Geophys. Res.* **109**, E07001 (2004).
70. T.L. Jackson, W.M. Farrell, *IEEE Trans. Geosci. Remote Sensing* **44**, 2942 (2006).
71. E. Williams, N. Nathou, E. Hicks, C. Pontikis, B. Russell, M. Miller, M.J. Bartholomew, *Atmos. Res* **91**, 292 (2009).
72. A.R. Johnston, H. Kirkham, *IEEE Trans. Power Deliv.* **4**, 1253 (1989).
73. N.O. Renno, J.F. Kok, H. Kirkham, S. Rogacki, *J. Phys.: Conf. Ser.* **142**, 012075 (2008).
74. X. Zheng, L. He, Y. Zhou, *J. Geophys. Res.* **109**, D15208 (2004).
75. N. Huang, G. Yue, X. Zheng, *J. Geophys. Res.* **113**, D20203 (2008).
76. Y. Shao, M.R. Raupach, *J. Geophys. Res.* **97**, 20559 (1992).
77. I. Delgado-Fernandez, *Aeolian Res.* **2**, 61 (2010).
78. D.W. Fryrear, A. Saleh, *Soil Sci.* **161**, 398 (1996).
79. D.A. Gillette, G. Herbert, P.H. Stockton, P.R. Owen, *Earth Surf. Process. Landf.* **21**, 641 (1996).
80. Z. Dong, H. Wang, X. Liu, X. Wang, *Geomorphology* **57**, 117 (2004).
81. A.C.W. Baas, D.J. Sherman, *J. Geophys. Res. F* **110**, F03011 (2005).
82. H. Zhang, T.L. Bo, W. Zhu, X.J. Zheng, *J. Geophys. Res. Atmos.* **118**, 4494 (2013).
83. R.A. Bagnold, *The Physics of Blown Sand and Desert Dunes* (Methuen, London, 1941).
84. Y. Shao, *Physics and Modelling of Wind Erosion* (Springer, Berlin, 2008).
85. P.R. Owen, *J. Fluid Mech.* **20**, 225 (1964).
86. R.S. Anderson, P.K. Haff, *Science* **241**, 820 (1988).
87. B.T. Werner, *J. Geol.* **98**, 1 (1990).
88. Y. Shao, A. Li, *Boundary-Layer Meteorol.* **91**, 199 (1999).
89. R. Greeley, J.D. Iversen, *Wind as a geological process: On Earth, Mars, Venus, and Titan* (Cambridge University Press, New York, 1985).
90. N. Huang, X.J. Zheng, Y.-H. Zhou, R.S. Van Pelt, *J. Geophys. Res.* **111**, D20201 (2006).
91. J.F. Kok, N.O. Renno, *J. Geophys. Res.* **114**, D17204 (2009).
92. G. Yue, X.J. Zheng, *J. Geophys. Res.* **111**, D16106 (2006).
93. X.J. Zheng, L.H. He, J.J. Wu, *J. Geophys. Res.* **109**, B01106 (2004).
94. J.F. Kok, N.O. Renno, *Geophys. Res. Lett.* **33**, L19S10 (2006).
95. K.R. Rasmussen, J.F. Kok, J.P. Merrison, *Planet Space Sci.* **57**, 804 (2009).
96. T. Pahtz, H.J. Herrmann, T. Shinbrot, *Nat. Phys.* **6**, 364 (2010).
97. S. Haddad, M.J.H. Salman, R.K. Jha, *Proc. URSI Commission F Symposium, Louvain-la-Neuve, Belgium*, SP-194 (ESA Publications, 1983) p. 153.
98. X.C. Li, L. Xie, X.J. Zheng, *J. Quantum. Spectrosc. Radiat. Transf.* **113**, 251 (2012).
99. Y.D. Fan, P.J. Shi, X. Wang, Y.Z. Pan, *Adv. Earth Sci. (Chinese)* **17**, 289 (2002).
100. K.B. Mao, Z.H. Qin, M.C. Li, B. Xu, *Remote Sensing Inform (Chinese)* **3**, 63 (2005).
101. J. Huang, P. Minnis, Y. Yi, Q. Tang, X. Wang, Y. Hu, Z. Liu, K. Ayers, C. Trepte, D. Winker, *Geophys. Res. Lett.* **34**, L18805 (2007).
102. J.P. Huang, Z.W. Huang, J.R. Bi, W. Zhang, L. zhang, *Atmos. Oceanic Sci. Lett.* **1**, 8 (2008).
103. J.M. Ge, Y.Z. Liu, J.P. Huang, J. Su, J.M. Li, J.R. Bi, *J. Appl. Opt. (Chinese)* **30**, 202 (2009).
104. X. Li, X.C. Li, X.J. Zheng, *Appl. Opt.* **49**, 6756 (2010).



Xiaojing Zheng, President of Xidian University, Professor in the Department of Mechanics of Lanzhou University, China, Member of CAS and TWAS, Regional Editor of *Computers, Materials & Continua*, Chief-editor of *Acta Solid Mechanica Sinica*, etc. Besides the electrification of wind-blown sand, her recent studies have focused on 3D real-time measurements of the turbulent structures of near-surface wind-blown sand flows and dust storms, and successfully realized quantitative simulations on the evolution of dune fields. She has published 150 papers and 3 academic books, in which *Mechanics of Wind-Blown Sand Movements* was collected into *Environmental Science and Engineering Series* by Springer-Verlag.